

Title	Active-mode CAOS camera demonstration
Authors	Riza, Nabeel A.;Mazhar, Mohsin A.
Publication date	2020-07-29
Original Citation	Riza, N. A. and Mazhar, M. A. (2020) 'Active-Mode CAOS Camera Demonstration', IEEE Photonics Technology Letters, doi: 10.1109/LPT.2020.3012867
Type of publication	Conference item
Link to publisher's version	https://ieeexplore.ieee.org/abstract/document/9152005 - 10.1109/LPT.2020.3012867
Rights	© 2020 IEEE. Personal use of this material is permitted. Permission from IEEE must be obtained for all other uses, in any current or future media, including reprinting/republishing this material for advertising or promotional purposes, creating new collective works, for resale or redistribution to servers or lists, or reuse of any copyrighted component of this work in other works.
Download date	2023-05-05 01:59:04
Item downloaded from	http://hdl.handle.net/10468/10353

Active-Mode CAOS Camera Demonstration

Nabeel A. Riza, *Fellow, IEEE*, and Mohsin A. Mazhar

Abstract— For the first time, demonstrated is the active-mode CAOS (i.e., Coded Access Optical Sensor) camera. The design demonstrated uses a hybrid approach to both optical device engagement and time-frequency CAOS mode operations. Specifically, time-frequency modulation of both the target illumination light source and the Digital Micromirror Device (DMD) combine to deliver the Frequency Modulation (FM)-Code Division Multiple Access (CDMA) mode of the CAOS camera. Using a 39.6 Klux white light 32 KHz FM LED source combined with a 1 KHz bit rate 4096 bits Walsh sequence CDMA code via the DMD, achieved is 58 x 70 CAOS pixels near 60 dB linear Dynamic Range (DR) imaging of a 36 patch calibrated high DR white light target. Applications for the active-mode CAOS camera are numerous and includes indoor full spectrum food inspection and photography where a linear DR camera can play an important role for accurate analysis and color image recovery.

Index Terms— Camera, Digital Micromirror Device, Optical Imaging, Optical MEMS, Imager Design

I. INTRODUCTION

CERTAIN scenarios across various applications require a full spectrum high linear DR camera to enable robust decision making to meet critical system requirements. These applications with spectral wavelengths over 400 nm to 2500 nm and a linear DR ≥ 60 dB include industrial testing during food inspection to laser manufacturing operations to robotic vision systems for precision guidance control. Although CCD and CMOS silicon sensor-based camera systems dominate the restricted visible band landscape and in many cases deliver excellent performance when considering pixel size, pixel count, frame rate, power consumption and size/weight metrics [1,2], recent experiments in the visible band indicate a limited recovery of low contrast targets embedded within a high (e.g., 95 dB) linear DR scene [3]. Researchers, including in the last few years, continue to look for alternate ways to design improved camera systems such as via the use of tunable acousto-optic filters [4], Fabry-Perot tunable optical MEMS [5], MEMS arrays [6], coded apertures [7], digital MEMS-based computational methods [8-9], lenslet-based Fourier domain interferometry compressive sensing [10], and cryogenics [11]. These methods are not specifically motivated for enabling linear DR full spectrum camera responses.

To meet this need for full spectrum coverage from UV to visible to Near-IR with high linear DR image recovery focus, recently proposed is the CAOS camera that works on the principles of the extreme DR multi-access RF wireless mobile network [12-13]. The CAOS camera design engages cost effective optical and electronic technologies that for example includes electronic Digital Signal Processing (DSP) modules, high speed Analog-to-Digital Converters (ADC), high speed point Photo-Detectors (PDs), and DMD light modulation technology. Recent experiments have indeed shown the extreme linear DR imaging capability of the CAOS camera, reaching a 177 dB DR level [14]. Furthermore, CAOS camera experiments conducted so far operate using the passive mode of the CAOS camera where the camera images unmodulated direct or indirect target scattered light. For example, CAOS camera imaging of the Sun that is a natural unmodulated white light emitter [15].

Another powerful mode of the CAOS camera is the active light operations mode where a target to be imaged is illuminated by a CAOS time-frequency modulated coded light signal [12-13]. This *active-mode CAOS camera* forms a highly versatile linear high DR imaging platform with a precision controlled active light illumination source where depending on the imaging environment, the light power, exposure time and spectral content can be adjusted for optimal Signal-to-Noise Ratio (SNR) spectral response target imaging. This additional light control capability, whether indoor or outdoor can be highly useful in optimizing image recovery, including the use of infrared sources such as eye safe >1400 nm light. Hence, this letter presents the first demonstration of the active-mode CAOS camera. Specifically, a white light LED array target illumination source is engaged with a DMD-based CAOS camera design to demonstrate linear DR imaging of a high DR calibrated white light target. Explained next are the details of the camera experiment and its imaging results.

II. ACTIVE-MODE CAOS CAMERA

Fig.1 shows the top view of the demonstrated active-mode CAOS camera design. An external light source that is part of the proposed active-mode CAOS camera system is pointed in the direction of the target to be imaged. This active time-

frequency coded light source can take a variety of forms such as LED, laser, LED array, laser array, hybrid laser-LED array sources including fiber assembled and fed light sources that can be spatially controlled and time-frequency modulated. The target scattered/reflected/transmitted light travels to the CAOS camera A1 aperture and F1 filter before entering the imaging lens L1 that maps the target plane on to the DMD plane. Depending on the imaging scenario needs such as the required linear DR, the CAOS camera can operate with various time-frequency CAOS modes [16].

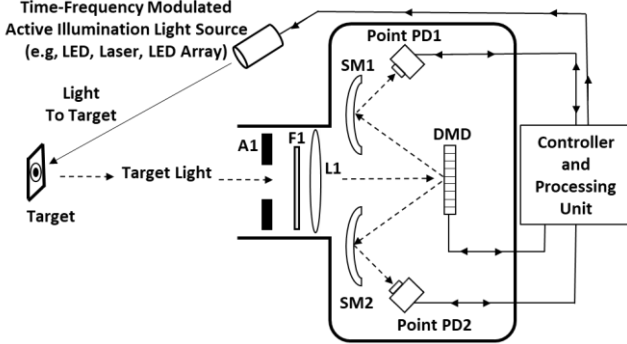


Fig. 1 Top view of the active-mode CAOS camera.

For the active-mode CAOS camera, the FM-CDMA mode is engaged where the external light source provides the FM coding while the DMD provides the CDMA coding for the simultaneously viewed M CAOS pixels. In the previously demonstrated passive-mode CAOS camera FM-CDMA mode [16], the DMD also provided the FM coding of the M pixel irradiances with the FM rate currently limited to 25 KHz given a 50 KHz DMD board manufacturer specified maximum DMD frame rate. The demonstrated active-mode CAOS camera FM-CDMA mode eliminates the 25 KHz FM restriction and shifts it to the active light source FM rate that can easily exceed 25 KHz to provide lower electronic noise and faster imaging rates, hence the proposed demonstration using an LED active light source. Additionally, compared to the DMD that implements a digital square wave FM that produces harmonics in the spectral space, an active light source such as LED or laser produced FM can deliver a pure sinusoidal FM carrier that does not generate harmonics that can cause crosstalk in the image pixels irradiance recovery. It is also important that the FM rate f_C Hz is greater than the CDMA bit rate f_B Hz so that multiple FM carrier cycles occur in a bit time to allow RF spectral processing of the FM carrier via the DSP Fast Fourier Transform (FFT) algorithm. A best practice design would be $f_C = f_B P$, where P is an integer. Because the DMD micromirrors operate as a two tilt state device, imaged light gets directed via spherical mirrors SM1 and SM2 to the point PDs labelled as PD1 and PD2. It is important to point out that any CAOS mode using the FM encoding technique allows one to engage an additional gain and filtering dimension, specifically, the spectral DSP gain via FFT

processing allowing higher dynamic range and improved SNR pixel irradiance extraction.

Imaging is preserved between the DMD and PD planes. The received FM-CDMA encoded RF signals from the point PDs carry the observed image M CAOS pixel irradiance data that enters a controller and processing unit containing ADC channels as well as DSP processors. Decoding of the FM-CDMA data via spectral and correlation processing recovers the viewed image [16,17]. On a design note, A1 and F1 can be electronically controlled and PD1 and PD2 can cover different spectral bands, e.g., PD1 a Silicon detector while PD2 a Germanium or InGaAs detector, giving 400 nm to 1700 nm full spectrum camera coverage [18]. In addition, during CAOS camera calibration operations using specified target DR values, deployed active source illumination light power levels should be measured and tabulated that provide the best DR recovery for a desired robust SNR given PD1/PD2 saturation limits as well as the electronic gain (e.g., 0 to 70 dB settings) and DSP gain settings deployed for low noise photo-detected signal recovery and image processing. The Field of View (FOV) of the camera is designed and limited based on the sizes of the A1 and DMD and L1 focal length. The camera imaging resolution depends on the size of the CAOS pixel which can be as small as one micromirror on the DMD. The number of CAOS pixels simultaneously seen depends on the bit length of the CDMA code deployed for multi-access CAOS implementation indicating a tradeoff between imaging time and number of CAOS pixels. Hence, based on the application, CAOS camera optical and electronic parameters must be selected to match the priorities of the imaging operation.

III. EXPERIMENTS AND DISCUSSION

The Fig.1 active-mode CAOS camera is built in the laboratory using the following components. Image Engineering (Germany) provided Custom 160 dB DR 36 patch target (see Fig.2 for design) and LG3 white light LEDs target illumination source, Vialux (Germany) DMD model V-7001, DELL 5480 Latitude laptop for control and DSP, National Instruments 16-bit ADC model 6366, and Thorlabs components that include silicon point PDs model PDA100A2, 5.08 cm diameter Iris A1, and 5.08 cm diameter 10 cm focal length front imaging lens L1, 5.08 cm diameter spherical mirrors SM1 and SM2 with 3.81 cm focal lengths. Inter-component distances are: 10.4 cm L1: DMD, 9.8 cm SM1/SM2:DMD, 6.3 cm SM1/SM2:PD1/PD2 and 261 cm target/L1. A factor of 25.1 demagnification takes place between target and DMD plane. F1 filter is not engaged for the experiment given gray-scale white light image target parameters. By using a single uncoated broadband imaging lens L1, maximum optical visible and near infrared spectrum transmission is achieved and use of non-color target leads to chromatic aberration having a limited effect on the overall imaging quality of the tested target camera. As shown in Fig.3, the deployed FM code within the CAOS FM-CDMA mode is a $f_C = 32$ KHz and 50% duty cycle square wave signal driving the

white light LEDs in LG3. The LG3 active source provides 39.5 Klux that illuminates the gray-scale calibrated 36-patch target. The CDMA mode via the DMD uses an $f_B = 1$ KHz giving $P=32$ cycles per CDMA code bit with a 4096 bits Walsh sequence providing $M= 58 \times 70$ CAOS pixels grid in the viewed image space.

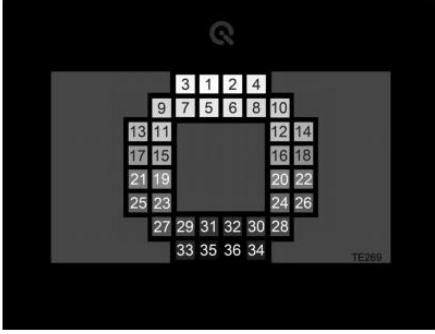


Fig. 2 Custom 36-Patch high DR target design with numbered patches.

The ADC sampling rate is 1 MSps with the point PD electronic gain set to 40 dB. The digitized FM-CDMA signal from the CAOS camera point PD1 first undergoes a $N=1024$ point FFT with a DSP FFT gain of $10\log(N/2)$ dB and then CDMA decoding via correlation processing to recover the scaled irradiance values for the observed $M = 4060$ CAOS pixels. Each CAOS pixel is made of 13×13 micromirrors where each micromirror is $13.68 \mu\text{m} \times 13.68 \mu\text{m}$. A single PD channel is used for image processing although 2 channels can also be used for dual spectrum [18] or lower noise differential processing [19].

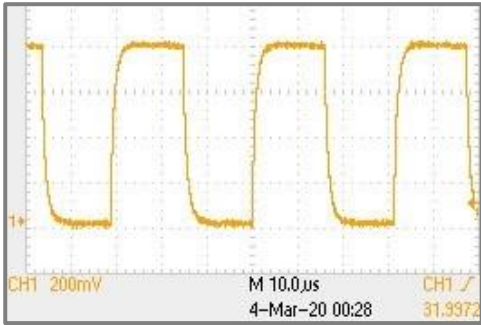


Fig. 3 Active-mode CAOS camera deployed 32 KHz FM signal CAOS code for the white LEDs-based 39.6 Klux source illuminating the target.

Note that the CAOS imaging measured DR for the n^{th} patch in $\text{dB} = 20 \log (P_1/P_n)$, where P_1 and P_n are the scaled optical power levels for Patch 1 (i.e., the brightest patch in the target) and Patch number n , respectively. $\text{SNR} = (\text{Scaled signal optical power of CAOS pixel}) / (\text{Scaled noise optical power of CAOS image Dark Pixel})$ and an $\text{SNR} = 1$ produces the maximum possible camera detection DR. The scaled noise optical power signal is computed from the CAOS camera imaged pixels without illumination, i.e., the black pixels. The LG3 illumination is controlled to a level of $1/4000$ or 0.25% and has

a $\geq 95\%$ uniformity in its white light illumination area. The CAOS camera captured both the white illumination zone inside the field-of-view of the camera as well as the surrounding light-free black area (see Fig.4). Data analysis of the Fig.4 image shows a measured uniformity of 95% with a measured average scaled illumination value of 0.76 on a zero to 1 scale.

With the 36-patch target illuminated by the active source with a 32 KHz FM-code and 1 KHz CDMA-code, Fig.5 shows the CAOS FM-CDMA mode recovered 14 target patches indicating a 59.4 dB DR recovery with an $\text{SNR} > 1$ (see Table 1 where M (dB) column gives the CAOS camera measured DR for a given test patch number). The DR value for Patch 1 associated with the brightest patch is 0 dB. The scaled optical power level used in the DR computation for each patch is calculated by taking the mean of the measured scaled optical power values of the 9 brightest CAOS pixels in the $4 \times 4 = 16$ CAOS pixels grid used to image each patch. Fig.6 shows the image recovery is linear over this range with a fitted slope of 0.94 versus the ideal slope of 1.

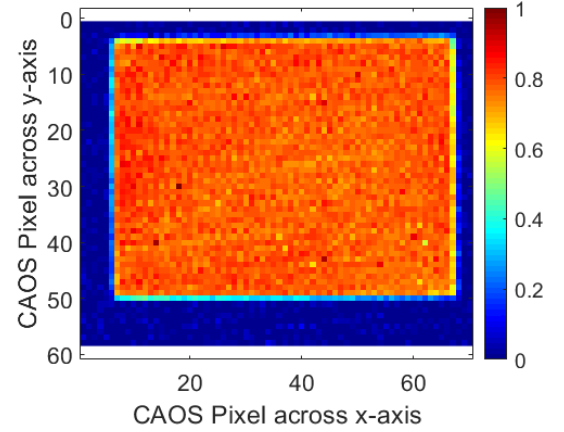


Fig. 4 Active-mode CAOS camera generated image of the LG3 active light source illumination at target screen location without the 36-patch target. Image shown in a 0 to 1 linear scale.

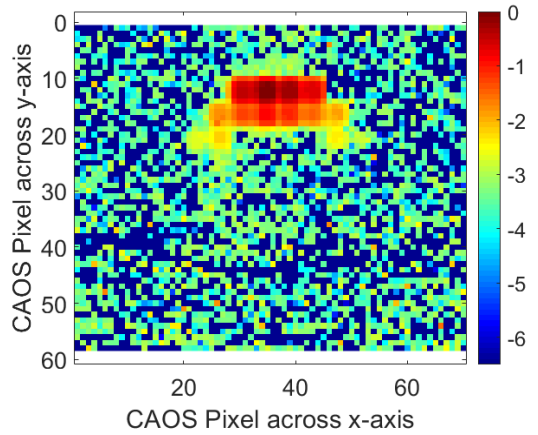


Fig. 5 Active-mode CAOS Camera generated near 60 dB DR image of the Fig.2 36-patch target. The camera used its FM-CDMA mode. Image shown in log scale in order to display a high DR on a computer screen.

TABLE 1
ACTIVE-MODE CAOS CAMERA MEASURED TARGET PATCH DR VALUES

Patch #	DR (dB)	M (dB)	SNR	Patch #	DR (dB)	M (dB)	SNR
1	- (ref)	-	836.7	8	32	30.0	26.6
2	4.6	4.2	516.8	9	36.6	34.0	16.8
3	9.2	8.9	301.9	10	41.2	37.5	11.2
4	13.8	12.5	198.3	11	45.8	44.5	5.0
5	18.2	17.1	117.4	12	50.2	48.4	3.2
6	22.8	21.5	70.7	13	54.8	52.4	2.0
7	27.4	26.0	42.1	14	59.4	55.3	1.4

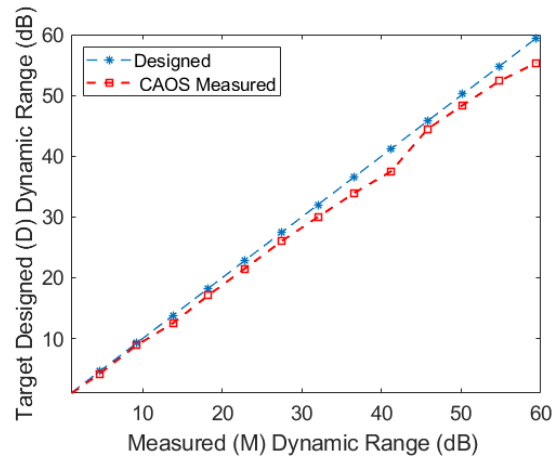


Fig. 6 Linearity plot for the active-mode CAOS camera image data.

IV. CONCLUSION

For the first time, demonstrated is the active-mode CAOS camera that is empowered by an external light source that implements part of the CAOS camera light encoding operations. Compared to the passive-mode CAOS camera, the active-mode CAOS camera features additional flexibility to optimize linear DR imaging via illumination power as well as spatial and temporal/frequency higher FM rate control to empower higher DR lower noise imaging. Experiments indeed show near 60 dB linear DR white light imaging via LED-based illumination that implements the FM-mode while the DMD implements the CDMA-mode of the CAOS camera to complete CAOS FM-CDMA mode imaging of a high DR calibrated target. An interesting extension of the active-mode CAOS camera is the use of a structured spatial pattern projected on the target that can be used for target depth mapping [13, 20]. The active-mode CAOS camera can be used for various indoor and out-door imaging applications that require a linear DR and full spectrum coverage within one cost-effective camera unit. Example applications include robust measurements of white light scenes requiring accurate calibrations such as in food inspection analysis and color photography for artifacts.

REFERENCES

- [1] G.C. Holst, and T. S. Lomheim, "Introduction," in *CMOS/CCD Sensors and Camera Systems*, 2nd ed., vol. PM208, SPIE Press, 2011 pp. 1-18
- [2] J. Ohta, "Introduction" in *Smart CMOS image sensors and applications* 1st ed., CRC Press, 2007, pp. 1-11.
- [3] N. A. Riza, and M. A. Mazhar. (2020, January). Robust Low Contrast Image Recovery over 90 dB Scene Linear Dynamic Range using CAOS Camera. IS & T 2020 Electronic Imaging Conf. Proc. Available: <https://www.ingentaconnect.com/content/ist/ei/pre-prints/content-ei2020-iss-226>.
- [4] R. Abdlaty, J. Orepoulos, P. Sinclair, R. Berman, Q. Fang, "High Throughput AOTF Hyperspectral Imager for Randomly Polarized Light," *Photonics*, vol. 5, no.3, pp. 1-10, Jan. 2018.
- [5] A. Näsälä et al., (2019, Mach). Cubic-inch MOEMS spectral imager. Proc. SPIE, MOEMS and Miniaturized Systems XVIII. Available: <https://doi.org/10.1117/12.2508420>
- [6] J. Roul, F. Blanc, S. Lacroix, and A. Monmayrant. (2017, June). Co-design of an adaptive hyperspectral imager based on MEMS arrays: From proof of principle to a research prototype. 2017 Symposium on Design, Test, Integration and Packaging of MEMS/MOEMS (DTIP). Available: <https://ieeexplore.ieee.org/document/7984470>
- [7] L. Pei, Q. Lv, Y. Liu, J. Wang. (2017, Oct). Optical system design of the coded aperture super-resolution imager. Proc. SPIE Sensors, Systems, and Next-Generation Satellites XXI. Available: <https://doi.org/10.1117/12.2280401>
- [8] Y. Qi et al. (2019, July). A Single-Pixel Hyperspectral Imager based on Digital Micromirror Device. Proc. IEEE. 2019 International Conference on Optical MEMS and Nanophotonics (OMN). Available: <https://ieeexplore.ieee.org/document/8925274>
- [9] Y. Qi et al., "A single-pixel hyperspectral imager using two-stage Hadamard encoding," *Opt. Commun.*, vol. 470, pp. 1-10, Sept. 2020.
- [10] G. Liu, D. Wen, Z. Song, Z. Li, W. Zhang, and X. Wei, "Optimized design of an emerging optical imager using compressive sensing," *Opt. Laser Technol.*, vol. 110, pp. 158-164, Feb. 2019.
- [11] L. Li. (2018, Feb). The design and application of a multi-band IR imager. Proc. SPIE, Fourth Seminar on Novel Optoelectronic Detection Technology and Application. Available: <https://doi.org/10.1117/12.2310116>
- [12] Coded Access Optical Sensor (CAOS), N. A. Riza (2019, July). Patent 10356392 B2. Available: <https://patents.google.com/patent/US10356392B2/en?q=10356392++>
- [13] N. A. Riza, M. J. Amin, and J. P. La Torre, "Coded Access Optical Sensor (CAOS) Imager," *JEOS Rapid Publications*, vol. 10, pp. 150211-8, 2015. DOI: [10.2971/jeos.2015.15021](https://doi.org/10.2971/jeos.2015.15021)
- [14] N. A. Riza, and M. A. Mazhar, "177 dB Linear Dynamic Range Pixels of Interest DSLR CAOS Camera," *IEEE Photonics J.*, vol. 11, no. 3, pp. 1-10, June. 2019. DOI: [10.1109/JPHOT.2019.2909430](https://doi.org/10.1109/JPHOT.2019.2909430)
- [15] N. A. Riza, M. A. Mazhar, and N. Ashraf (2020, September), Solar Limb Darkening Color Imaging of the Sun with the Extreme Brightness Capability CAOS Camera, IS & T London Imaging Meeting Conf.
- [16] N. A. Riza, and M. A. Mazhar, "Laser beam imaging via multiple mode operations of the extreme dynamic range CAOS camera", *Appl. Opt.*, vol. 57, no. 22, pp. E20-E31, June, 2018.
- [17] N. A. Riza, and M. A. Mazhar, "Demonstration of the CDMA-mode CAOS smart camera", *Opt. Express*, 2017, vol. 25, no. 25, pp.31906-31920, Dec. 2017. DOI: [10.1364/OE.25.031906](https://doi.org/10.1364/OE.25.031906)
- [18] N. A. Riza, and M. A. Mazhar, (December, 2018). The CAOS Camera – Unleashing the Power of Full Spectrum Extreme Linear Dynamic Ranging Imaging. 1st IEEE BICOP Conf. Proc., Available: <https://ieeexplore.ieee.org/document/8658317>
- [19] N. A. Riza, and M. J. Mughal, "Optical Power Independent Optical Beam Profiler", *Opt. Eng.*, vol. 43, no. 4, pp. 793-797, Apr. 2004.
- [20] N. A. Riza, (September, 2020), Thinking Camera – Powered by the CAOS Camera Platform Proc. of European Optical Society Annual Meeting (EOSAM)